Draft genomes of the three northern hemisphere blue mussel lineages: North and South European *Mytilus edulis* and Mediterranean *Mytilus galloprovincialis*.

Alexis Simon[1,*], Christine Arbiol[1], and Nicolas Bierne[1]

[1]CNRS, Univ Montpellier, . . .

June 29, 2022

Abstract

Using the 10X chromium long reads technology, we provide draft genomes for three closely related blue mussel species from the *Mytilus* species complex. The objective was to produce affordable genomic resources for population and evolutionary genomic studies. Genomes are fragmented but represent a large portion of the genome, with good sizes and BUSCO scores.

Keywords: *Mytilus edulis*, *Mytilus galloprovincialis*, Genome assembly, 10X chromium

* **Corresponding author**: alexis.simon@normalesup.org

1 Rationale and objectives

The *Mytilus* species complex has been a model system in population genetics, adaptation, hybridization and speciation since genetic variants could be identified (Ahmad et al., 1977; Bierne et al., 2003; Fraïsse et al., 2016; Koehn & Mitton, 1972; Milkman & Beaty, 1970; Quesada, Wenne, et al., 1995; Simon et al., 2021; Skibinski et al., 1978).

The *Mytilus* species complex is composed of three taxonomically recognized and partially reproductively isolated species in the northern hemisphere, *Mytilus edulis*, *M. galloprovincialis* and *M. trossulus*. Within each species, evolutionary relevant lineages can be identified. Two lineages of *M. galloprovincialis* can be identified, one Atlantic lineage and one Mediterranean lineage separated by a hybrid zone along the Almeria-Oran front (El Ayari et al., 2019; Fraïsse et al., 2016; Quesada, Zapata, et al., 1995). Three lineages of *M. edulis* can be identified: (i) an American lineage, (ii) a Southern European lineage, and (iii) a Northern European lineage (Fraïsse et al., 2016; Simon et al., 2020).

As an effort to diversify the genomic resources available for the *Mytilus* species complex, we assembled and annotate the genomes of three lineages using the 10X chromium technology. While our assemblies were initially fragmented due to the high level of heterozygosity, we leveraged the existence of a chromosome scale assembly of a sister species to scaffold our assemblies against it. We obtained assemblies equivalent to published ones in term of completeness for three new lineages of the species complex using a low sequencing budget and publicly available data. The resources produced and the assembly pipeline are freely available for use by the community.

2 Methods

General notes: The entire assembly was carried out using a Snakemake (Mölder et al., 2021) pipeline available on github at https://github.com/alxsimon/assembly_10x. Where deemed important, parameters are given in the text. For brevity and simplicity, not all information might be available in the text. However, all parameters, software versions and steps are retrievable from the repository.

Important caveat: The assembled genome of MeduEUN (*M. edulis* Northern lineage) was initially thought to be *M. trossulus*. Therefore some assembly and annotation steps wrongly used *M. trossulus* transcriptomes. While this is not ideal, we think results have not been strongly impacted by this issue.

2.1 Biological material and DNA extraction

One individual for each species of interest was collected and processed fresh.

Collection locations:

- *M. galloprovincialis* Mediterranean MgalMED; Sète, France

- *M. edulis* Southern European MeduEUS; ???

- *M. edulis* Northern Europe MeduEUN; ???

52 Whole mussels were placed in 50 mL falcon tubes containing 25 ml of TNES-Urea
53 solution and incubated for 4-6 weeks at room temperature (TNES-Urea: 10 mM Tris-HCl
54 pH 7.4; 120 mM NaCl; 10 mM EDTA pH 8.0; 0.5% SDS; 4 M urea).

55 After this period of pre-treatment at ambient temperature, proteinase K was added at a
56 final concentration of 150 μg/mL and the solution was incubated overnight at 56řC.

57 High Molecular weight genomic DNA was extracted following Nakayama et al. (1994).
58 We used a 15 mL Phase Lock Gel Heavy extraction with 3 steps of phenol / chloroform
59 / isoamylalcool (25/24/1) Tris pH 8,1 followed by 2 chloroform extractions. After the last
60 extraction, the aqueous supernatant was precipitated with 2 volumes of 100% EtOH and the
61 pellet was hooked from the solution with a sterile glass Pasteur pipette. The pellet was
62 rinsed several times in 80% EtOH before being dried at room temperature.

63 DNA was resuspended with an appropriate volume of biomolecular water at 65řC for
64 several hours, the duration of this incubation depending on the size of the granules. DNA
65 was then stored at 4řC.

66 Prior to the construction of the DNA libraries, DNA was repaired with NEBNext FFPE
67 DNA Repair Mix according to the manufacturer's instructions.

2.2 Library preparation and sequencing

69 The 10X chromium library preparation and sequencing was subcontracted to the MGX plat-
70 form (Montpellier, France). The 10X linked reads libraries for each individual were pro-
71 duced following the 10X Genomics Genome Reagen Kit (*Genome Solution*) protocol using a
72 Chromium microfluidic chip. Libraries were subsequently sequenced on an Illumina NovaSeq
73 6000 with an S4 flowcell.

2.3 Preprocessing 10X reads

75 We preprocessed 10X reads using the following pipeline for use in several algorithms (sec-
76 tion 2.4). We first removed duplicate reads using `Nubeam-dedup` (Dai and Guan, 2020; com-
77 mit 25dd385). We then used `proc10xG` (https://github.com/ucdavis-bioinformatics/proc10xG;
78 commit 7afbfcf) to split the reads from their 10X barcodes for further processing. We
79 used a custom filtering step designed to remove under- and over-represented barcodes
80 and their associated reads from the data (figs. S1 to S3, `filter_barcodes.R` script, see
81 **Bary"&Gagnaire??**). Reads were additionally filtered with `fastp` (v0.20.1; Chen et al.,
82 2018) with the main objective to remove poly-G tails created by the Illumina Novaseq se-
83 quencing technology. We obtained at this point reads equivalent to a short-read sequencing
84 run, usable in some parts of the assembly and quality control pipeline. Additionally, to obtain
85 reads compatible to 10X genomics tools, we filtered and reassembled reads with their 10X
86 barcodes in `proc10xG` using the `filter_10xReads.py` and `regen_10xReads.py` scripts.

2.4 Initial genome assemblies

88 For each genome we used `Supernova` v2.1.1 (Weisenfeld et al., 2017) to assemble raw 10X
89 reads. To avoid hard stops in `Supernova` due to both data quantity slightly under 10X
90 genomics recommendations and an overestimation of genome size by Supernova, we used all
91 available reads (`--maxreads='all'`) and accepted extreme coverage (`--accept-extreme-coverage`).

We produced every style of Fasta output available in `Supernova` but only used the pseudo-haploid output in the following pipeline.

To remove duplicate haplotypes in the assemblies, we followed the `purge_dups` pipeline (Guan et al., 2020; commit e1934bb). We first used the `longranger` v2.2.2 align algorithm to map preprocessed reads (section 2.3) to the pseudo-haploid genomes to use in the `ngscstat` step. `Minimap2` (v2.17; Li, 2017) was used in the contig self-mapping step. We obtained the purged assemblies using the `get_seqs` steps without restricting the purging to the end of contigs (without the `-e` option).

We used `AGOUTI` (https://github.com/svm-zhang/AGOUTI; commit a7e65d6; Zhang et al., 2016) to improve scaffolding by using paired end RNA-seq reads. For each species, a different set of published transcriptomes were used (See Supplementary File 1 for accession numbers). `AGOUTI` require a gene prediction as input in addition to RNA-seq reads. We used `Augustus` (v3.3.3; Stanke et al., 2008) to produce an intermediate annotation for each assembly using the *Caenorhabditis* model. RNA-seq reads were first cleaned using `rcorrector` (v1.0.4; Song and Florea, 2015) and `trimgalore` (v0.6.6; https://www.bioinformatics.babraham.ac.uk/projects/trim_galore; `--quality 20 --stringency 1 -e 0.1 --length 70`). RNA-seq reads were mapped independently using `bwa-mem2` (v2.2.1; Vasimuddin Md et al., 2019), and then merged as a common bam file for each assembly with `samtools` (v1.12; Li et al., 2009). Finally, the `AGOUTI` scaffolding pipeline was run using the gene prediction and mapped RNA-seq reads (`-minMQ 20 -maxFracMM 0.05`; using `python` v2.7.15 and `samtools` v1.10 for compatibility).

As a last step, we ran `Blobtoolkit` (v2.4.0; Challis et al., 2020) on the three assemblies to evaluate quality and potential contamination levels. We used a custom script (`btk_conta_extraction.py`) to filter the assembly contigs based on the taxids found by the `Blobtoolkit` pipeline to remove the most obvious contaminations. Contigs matching taxids associated with viruses, bacteria and non-mollusca eukaryotes were removed. More specifically contigs for were removed for virus contamination if they presented a hit percentage of more than 10 % of their length. Contigs were removed for eukaryote contamination only when presenting only hits to taxa outside Mollusca on more than 10 % of their length. The list of retained contigs was used to filter the fasta assembly file using `seqkit` (v0.13.2; Shen et al., 2016).

2.5   Scaffolding on the *Mytilus coruscus* genome

At the time of assembly, the closest relative of the *Mytilus* species of interest with a chromosome scale assembly was *Mytilus coruscus* (GCA_017311375.1; Yang et al., 2021). Given the conserved number of 14 chromosomes in the *Mytilus* genus, we decided to scaffold our contigs on this high quality reference. Additionally, we had Oxford Nanopore reads for the MeduEUN individual. We used `minimap2` (v2.17; Li, 2017) and `LRScaf` (v1.1.10; https://github.com/shingocat/lrscaf) to first improve the MeduEUN assembly with this small amount of long reads.

Then for each assembly, we ran the scaffolder `RagTag` (v1.1.1; Alonge et al., 2021) to position contigs on the *M. coruscus* chromosomal assembly.

A final polishing step was performed using `Pilon` (v1.24; Walker et al., 2014). `Pilon` attempts to improve the assembly based on mapped read information (gap filling and error corrections). We used `bwa-mem2` to map the debarcoded and filtered 10X reads (section 2.3). In addition, Oxford Nanopore reads for MeduEUN were also used in `Pilon` for the given

137 assembly.

2.6 Repeats

139 We masked repeats for the purpose of annotation using `RepeatModeler` (v2.0.1; Flynn et al.,
140 2020) and `RepeatMasker` (v4.1.2–p1; Smit et al., 2013–2015) through the TETools DFAM
141 container (v1.3.1; https://hub.docker.com/r/dfam/tetools). We first built repeat databases for
142 each of five assemblies MgalMED, MeduEUS, MeduEUN, *M. coruscus* (GCA_017311375.1;
143 Yang et al., 2021) and *M. galloprovincialis* from the Atlantic (GCA_900618805.1; Gerdol
144 et al., 2020). Then, we built a common *Mytilus* database of repeats by merging those five
145 databases using `cd-hit` (v4.8.1; Fu et al., 2012). We used the same options as used by
146 default in `RepeatModeler`: `-aS 0.8 -c 0.8 -g 1 -G 0 -A 80 -M 10000`. Finally, soft
147 repeat masking was performed on the assemblies with `RepeatMasker` using the merged
148 database.

2.7 Annotation

150 We used `Braker2` (v2.1.6; Brna et al., 2021) as to obtain structural annotations, using both
151 a protein database and RNA–seq reads (preprocessed in section 2.4). To build the protein
152 database, we used all *Mollusca* proteins (taxid 6447) from OrthoDB (v10.1; Kriventseva et
153 al., 2019). To provide gene presence hints, we mapped all RNA–seq reads for each species
154 using `HISAT2` (v2.2.1; Kim et al., 2019).

155   We used the `Mantis` pipeline (https://github.com/PedroMTQ/mantis; commit c6cb597;
156 Queirós et al., 2021) to obtain consensus functional annotations of genes based on multiple
157 databases. Protein sequences for each assembly were built from the `Braker2` annotation
158 using the `python` module `gff3tool` (v2).

2.8 NCBI submission

160 The NCBI submission process identified a few errors that needed correcting. A small num–
161 ber of adaptor sequences and duplicates were removed to comply with NCBI requirements
162 (see the rule `ncbi_submission_changes.smk` in the pipeline for more details). Assem–
163 blies are available under the following accessions: JAKGDF000000000 for MgalMED,
164 JAKGDG000000000 for MeduEUS, and JAKGDH000000000 for MeduEUN.

2.9 Quality assessments and comparisons

166 Preprocessed 10X reads (section 2.3) were used to first estimate estimate genome size and
167 heterozygosities of the three individuals. We used the reference free k–mer based method
168 `GenomeScope` (https://github.com/tbenavi1/genomescope2.0; commit 5034ed4; Ranallo–Benavidez
169 et al., 2020) and the fork of the `KMC` k–mer counting program (https://github.com/tbenavi1/
170 KMC; commit 1df71f6).

171   Assembly statistics were computed with the `python` module `assembly_stats` (v0.1.4;
172 Trizna, 2020).

173   To assess the remaining level of duplication in the assemblies, we used the program `KAT`
174 (v2.4.2; Mapleson et al., 2017) to compare k–mer spectra from reads (preprocessed 10X) and
175 from the assembly.

176 Finally, gene completion analyses were carried out using `BUSCO` (v5.1.1; Manni et al.,
177 2021). We used both a Metazoan (`metazoa_odb10.2021-02-24`) and Molluscan (`mollusca_odb10.2020-08-05`)
178 database to assess and compare new and published assemblies. We compared our assem-
179 blies to the following published ones:

180 • *M. coruscus*, GCA_017311375.1, Yang et al. (2021);

181 • *M. galloprovincialis* from the Altantic lineage, GCA_900618805.1, Gerdol et al. (2020);

182 • *M. edulis* from the Southern European lineage, GCA_905397895.1, Corrochano-Fraile
183 et al. (2021)

184 • *M. edulis* from the American lineage, GCA_019925275.1.

185 ## 2.10 Phylogenetic species tree

186 We compiled protein sequences from published *Mytilus* genomes and transcriptomes, in
187 addition to the current three genomes and annotations, to build a species tree. We used
188 transcriptomes produced in Popovic and Riginos (2020) for American *M. edulis*, Mediter-
189 ranean *M. galloprovincialis*, *M. trossulus*, *M. californianus*. Transcriptomes were translated
190 using the `seqkit` program (v2.2.0; Shen et al., 2016) We used genomes and associated
191 annotations of *M. coruscus* (GCA_017311375.1; Yang et al. (2021)), Southern European *M.*
192 *edulis* (GCA_905397895.1; Corrochano-Fraile et al. (2021)), Atlantic *M. galloprovincialis*
193 (GCA_900618805.1; Gerdol et al. (2020)), and American *M. edulis* (GCA_019925275.1; an-
194 notation as personal communication of Tiago Hori, PEIMSO). For GCA_019925275.1, protein
195 sequences where retrieve from the fasta and gff files using the python module gff3tool (v2.1.0).

196 We used `OrthoFinder` (v2.5.4; Emms and Kelly, 2015, 2019) to find orthogroups and
197 orthologue genes. Species tree was inferred using the MSA method of `OrthoFinder` (Emms
198 & Kelly, 2018) using the `MAFFT` aligner (v7.505; Katoh and Standley, 2013), the `STRIDE`
199 species tree rooting algorithm (Emms & Kelly, 2017) and the `FastTree` software for tree
200 inference (v2.1.11; Price et al., 2009).

201 # 3 Results and discussion

202 ## 3.1 Assembly results

203 We introduce here newly assembled genomes from three lineages of the *Mytilus* species
204 complex. With a limited budget of $\sim$ 3000 per genome, we managed to produce draft
205 genomes of enough quality to be useful in applications such as population genomics and
206 genetics. The method of 10X chromium pseudo-long reads combined with scaffolding using
207 published data provided a quality comparable to published assemblies for *Mytilus* species.

208 The pre-assembly k-mer analysis carried out using GenomeScope (using 21-mers) showed
209 that, as expected, the genomes were highly heterozygous with values going from 3.49 to
210 8.77 % (fig. 1). For the MeduEUS data, GenomeScope provides a fit of bad quality and an
211 estimation probably off due to a reduced slightly lower sequencing depth compared to the
212 two other assemblies. In that case, the heterozygous peak was not identifiable.

213 Highly heterozygous genomes brings the risk of having a large number of duplicate
214 contigs due to the separate assembly of the two alleles from a same locus. For this reason,

we used the `purge_dups` pipeline to try removing a maximum of such bias. This procedure reduced the number of complete duplicated genes in all assemblies (fig. S5, v1 to v4). Overall, the compared `KAT` spectra analyses show that the assembly steps reduced the amount of duplication in all assemblies (fig. S4).
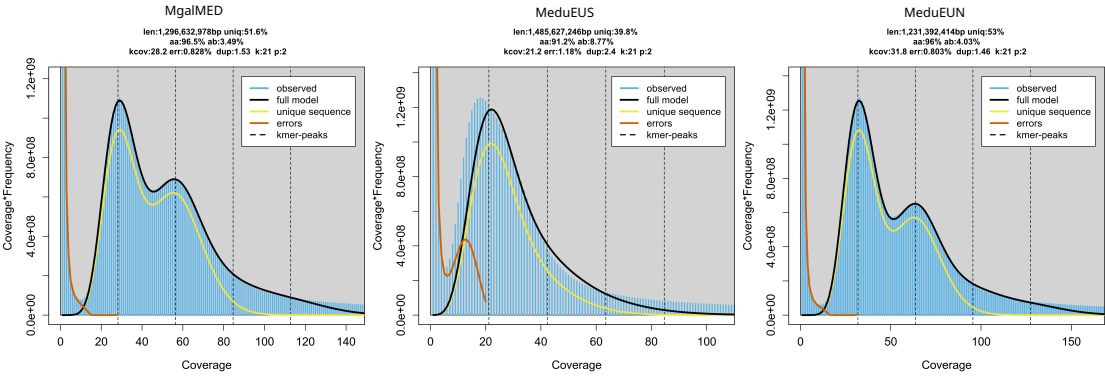
Figure 1: k–mer profile plots computed with 21–mers using GenomeScope. Coverage histogram of the k–mers in blue. Lines represent the fit of the GenomeScope models. len: inferred genome length; uniq: percentage of the genome that is unique, aa: overall homozygosity; ab: overall heterozygosity; kcov: mean k–mer coverage for heterozygous bases; err: reads error rate; dup: average rate of read duplication; k: k–mer size; p: ploidy.

Stats: GC contents: 32.1%, 34.6%, 32.1%

Table 1: Assembly statistics comparisons. C for contigs and S for scaffolds.

assembly	C.L50	C.N50	C.median	C.sequence_count	S.L50	S.N50	S.gc_content	S.median	S.sequence_count	S.total_bps
Mcor_GCA017311375	2.61×10^2	1.48×10^6	4.21×10^4	6449	6	9.95×10^7	32.4	2.13×10^4	4434	1.57×10^9
MgalATL_GCA900618805	4.92×10^3	7.70×10^4	3.95×10^4	22922	1903	2.08×10^5	32.1	7.76×10^4	10577	1.28×10^9
MeduEUS_GCA905397895	9.77×10^2	5.11×10^5	1.85×10^5	5966	464	1.10×10^6	32.2	2.92×10^5	3339	1.83×10^9
MeduAM_GCA019925415	8.35×10^2	4.91×10^5	6.25×10^4	9686	6	1.17×10^8	32.3	2.89×10^4	1119	1.65×10^9
MgalMED_v7	1.69×10^4	2.63×10^4	7.48×10^3	115913	9	7.20×10^7	32.1	4.53×10^3	41122	1.66×10^9
MeduEUS_v7	2.45×10^4	2.36×10^4	6.48×10^3	169324	415	2.28×10^5	34.6	5.00×10^3	73616	2.08×10^9
MeduEUN_v7	1.59×10^4	2.92×10^4	8.96×10^3	105892	9	7.71×10^7	32.1	6.16×10^3	28220	1.76×10^9

To assess the completeness of our assemblies, we compared them to four *Mytilus* published assemblies on the basis of a Metazoan and a Molluscan set of single copy orthologous genes using BUSCO (fig. 2). Overall, we show that our assemblies are equivalent to the published ones in terms of completeness.
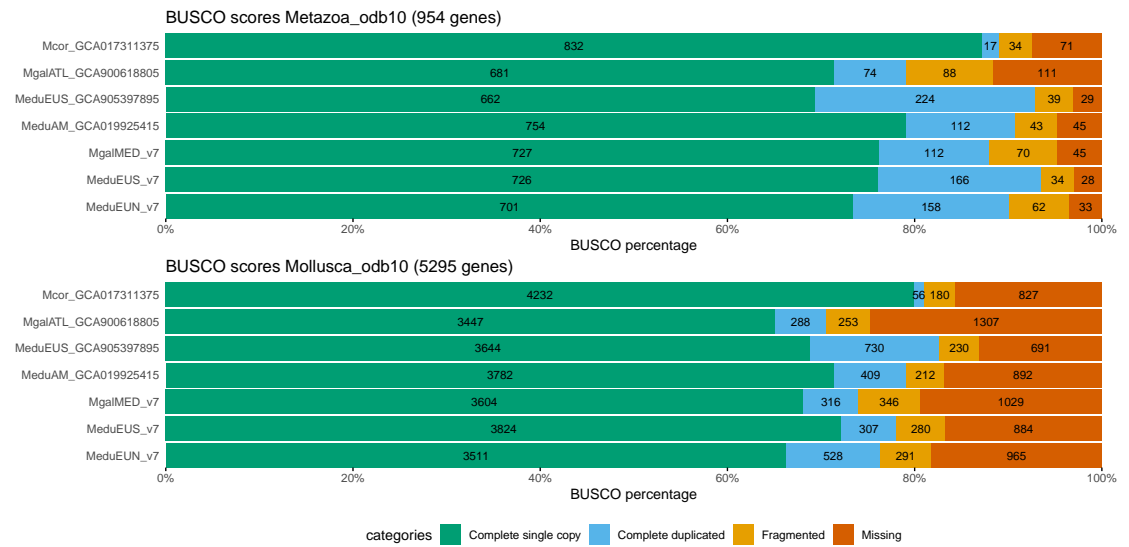

Figure 2: Busco scores

The MeduEUS assembly suffered from an increased level of contamination compared to the other two assemblies. Despite a broad contaminant filtering step, the Busco blob analysis (fig. S7) shows a second GC content peak centered around 40% (above the 32% peaks of this and other genomes).

3.2 Repeat contents

More than half of each genome was identified as repeats and masked by `RepeatMasker`. Repeats are estimated to amount to 57.22, 61.10 and 55.53% of the bases of MgalMED, MeduEUS and MeduEUN assemblies respectively. Table S2 gives the detailed proportions of repeats masked for the different types of repeats considered by the pipeline. The majority of repeats are unclassified, followed by retroelements with a balanced contribution of LINEs and LTR elements.

3.3 Annotations

[[Here goes annotation stats]]

3.4 Species tree

OrthoFinder assigned 499004 genes (91.9% of total) to 50543 orthogroups. Fifty percent of all genes were in orthogroups with 13 or more genes (G50 was 13) and were contained in the largest 11982 orthogroups (O50 was 11982). There were 1852 orthogroups with all species present and 173 of these consisted entirely of single-copy genes.

9

The species tree was built using 1300 orthogroups with a minimum of 81.8% of species having single-copy genes in any orthogroup (fig. 3). It shows that the assemblies and the published genomes and transcriptomes are clustering as expected.
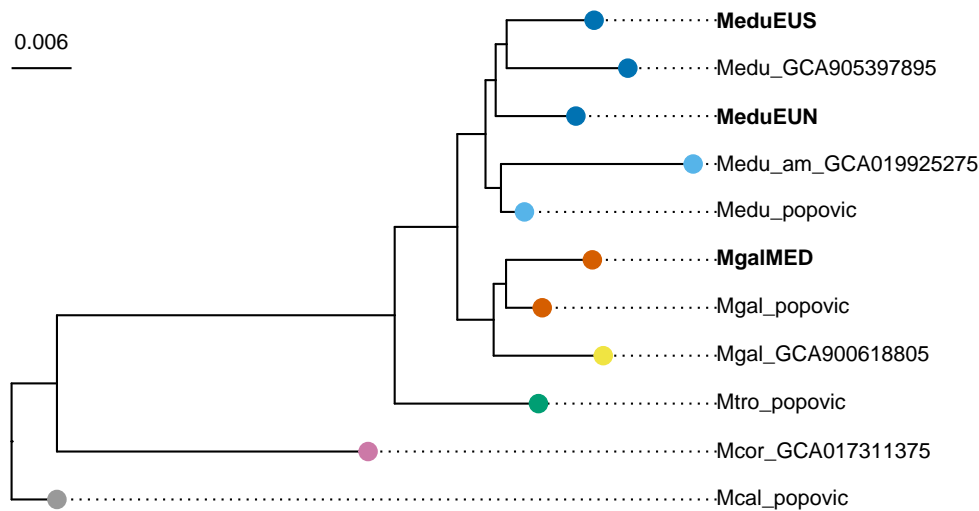
Figure 3: Species tree using 1300 orthogroups with a minimum of 81.8% of species having single-copy genes in any orthogroup. Color coding – dark blue: *M. edulis* Europe, light blue: *M. edulis* America, red: *M. galloprovincialis* Mediterranean Sea, yellow: *M. galloprovincialis* Atlantic, green: *M. trossulus*, pink: *M. coruscus*, gray: *M. californianus*.

Data availability

Raw data are available under BioProject PRJNA785550. Assemblies are available under accessions JAKGDF000000000 (MgalMED), JAKGDG000000000 (MeduEUS), and JAKGDH000000000 (MeduEUN). The assembly pipeline is available at https://github.com/alxsimon/assembly_10x. Annotations and the OrthoFinder pipeline and results are available on the Zenodo archive [[XXX]].

Acknowledgements

References

Ahmad, M., Skibinski, D. O. F., & Beardmore, J. A. (1977). An estimate of the amount of genetic variation in the common mussel Mytilus edulis. *Biochemical Genetics*, *15*(9-10), 833–846. https://doi.org/10.1007/BF00483980

261 Alonge, M., Lebeigle, L., Kirsche, M., Aganezov, S., Wang, X., Lippman, Z. B., Schatz, M. C.,
262   & Soyk, S. (2021). Automated assembly scaffolding elevates a new tomato system
263   for high-throughput genome editing. *bioRxiv*, 2021.11.18.469135. https://doi.org/10.
264   1101/2021.11.18.469135
265 Bierne, N., Borsa, P., Daguin, C., Jollivet, D., Viard, F., Bonhomme, F., & David, P. (2003).
266   Introgression patterns in the mosaic hybrid zone between *Mytilus edulis* and *M.
267   galloprovincialis*. *Molecular Ecology*, *12*(2), 447–461. https://doi.org/10.1046/j.
268   1365-294X.2003.01730.x
269 Brna, T., Hoff, K. J., Lomsadze, A., Stanke, M., & Borodovsky, M. (2021). BRAKER2: Automatic
270   eukaryotic genome annotation with GeneMark-EP+ and AUGUSTUS supported by
271   a protein database. *NAR Genomics and Bioinformatics*, *3*(1), lqaa108. https://doi.
272   org/10.1093/nargab/lqaa108
273 Challis, R., Richards, E., Rajan, J., Cochrane, G., & Blaxter, M. (2020). BlobToolKit Interactive
274   Quality Assessment of Genome Assemblies. *G3 Genes—Genomes—Genetics*, *10*(4),
275   1361–1374. https://doi.org/10.1534/g3.119.400908
276 Chen, S., Zhou, Y., Chen, Y., & Gu, J. (2018). Fastp: An ultra-fast all-in-one FASTQ prepro-
277   cessor. *Bioinformatics*, *34*, i884–i890. https://doi.org/10.1093/bioinformatics/bty560
278 Corrochano-Fraile, A., Davie, A., & Carboni, S. (2021). Evidence of multiple genome duplica-
279   tion events in Mytilus evolution. *bioRxiv*. https://doi.org/10.1101/2021.08.17.456601
280 Dai, H., & Guan, Y. (2020). Nubeam-dedup: A fast and RAM-efficient tool to de-duplicate
281   sequencing reads without mapping (I. Birol, Ed.). *Bioinformatics*, *36*(10), 3254–3256.
282   https://doi.org/10.1093/bioinformatics/btaa112
283 El Ayari, T., Trigui El Menif, N., Hamer, B., Cahill, A. E., & Bierne, N. (2019). The hidden
284   side of a major marine biogeographic boundary: A wide mosaic hybrid zone at the
285   AtlanticMediterranean divide reveals the complex interaction between natural and
286   genetic barriers in mussels. *Heredity*, *122*, 770–784. https://doi.org/10.1038/s41437-
287   018-0174-y
288 Emms, D. M., & Kelly, S. (2018). STAG: Species Tree Inference from All Genes. *bioRxiv*,
289   267914. https://doi.org/10.1101/267914
290 Emms, D. M., & Kelly, S. (2015). OrthoFinder: Solving fundamental biases in whole genome
291   comparisons dramatically improves orthogroup inference accuracy. *Genome Biology*,
292   *16*(1), 157. https://doi.org/10.1186/s13059-015-0721-2
293 Emms, D. M., & Kelly, S. (2017). STRIDE: Species Tree Root Inference from Gene Duplication
294   Events. *Molecular Biology and Evolution*, *34*(12), 3267–3278. https://doi.org/10.
295   1093/molbev/msx259
296 Emms, D. M., & Kelly, S. (2019). OrthoFinder: Phylogenetic orthology inference for compar-
297   ative genomics. *Genome Biology*, *20*(1), 238. https://doi.org/10.1186/s13059-019-
298   1832-y
299 Flynn, J. M., Hubley, R., Goubert, C., Rosen, J., Clark, A. G., Feschotte, C., & Smit, A. F.
300   (2020). RepeatModeler2 for automated genomic discovery of transposable element
301   families. *Proceedings of the National Academy of Sciences*, *117*(17), 9451–9457.
302   https://doi.org/10.1073/pnas.1921046117
303 Fraïsse, C., Belkhir, K., Welch, J. J., & Bierne, N. (2016). Local interspecies introgression is
304   the main cause of extreme levels of intraspecific differentiation in mussels. *Molecular
305   Ecology*, *25*(1), 269–286. https://doi.org/10.1111/mec.13299
306 Fu, L., Niu, B., Zhu, Z., Wu, S., & Li, W. (2012). CD-HIT: Accelerated for clustering the next-
307   generation sequencing data. *Bioinformatics*, *28*(23), 3150–3152. https://doi.org/10.
308   1093/bioinformatics/bts565

309 Gerdol, M., Moreira, R., Cruz, F., Gómez-Garrido, J., Vlasova, A., Rosani, U., Venier, P.,
310   Naranjo-Ortiz, M. A., Murgarella, M., Greco, S., Balseiro, P., Corvelo, A., Frias, L.,
311   Gut, M., Gabaldón, T., Pallavicini, A., Canchaya, C., Novoa, B., Alioto, T. S., . . .
312   Figueras, A. (2020). Massive gene presence–absence variation shapes an open pan-
313   genome in the Mediterranean mussel. *Genome Biology*, *21*(1), 275. https://doi.org/
314   10.1186/s13059-020-02180-3
315 Guan, D., McCarthy, S. A., Wood, J., Howe, K., Wang, Y., & Durbin, R. (2020). Identifying
316   and removing haplotypic duplication in primary genome assemblies. *Bioinformatics*,
317   *36*(9), 2896–2898. https://doi.org/10.1093/bioinformatics/btaa025
318 Katoh, K., & Standley, D. M. (2013). MAFFT Multiple Sequence Alignment Software Version
319   7: Improvements in Performance and Usability. *Molecular Biology and Evolution*,
320   *30*(4), 772–780. https://doi.org/10.1093/molbev/mst010
321 Kim, D., Paggi, J. M., Park, C., Bennett, C., & Salzberg, S. L. (2019). Graph-based genome
322   alignment and genotyping with HISAT2 and HISAT-genotype. *Nature Biotechnology*,
323   *37*(8), 907–915. https://doi.org/10.1038/s41587-019-0201-4
324 Koehn, R. K., & Mitton, J. B. (1972). Population Genetics of Marine Pelecypods. I. Ecolog-
325   ical Heterogeneity and Evolutionary Strategy at an Enzyme Locus. *The American
326   Naturalist*, *106*(947), 47–56. https://doi.org/10.1086/282750
327 Kriventseva, E. V., Kuznetsov, D., Tegenfeldt, F., Manni, M., Dias, R., Simão, F. A., & Zdobnov,
328   E. M. (2019). OrthoDB v10: Sampling the diversity of animal, plant, fungal, protist,
329   bacterial and viral genomes for evolutionary and functional annotations of orthologs.
330   *Nucleic Acids Research*, *47*(D1), D807–D811. https://doi.org/10.1093/nar/gky1053
331 Li, H., Handsaker, B., Wysoker, A., Fennell, T., Ruan, J., Homer, N., Marth, G., Abecasis,
332   G., Durbin, R., & 1000 Genome Project Data Processing Subgroup. (2009). The
333   Sequence Alignment/Map format and SAMtools. *Bioinformatics*, *25*(16), 2078–2079.
334   https://doi.org/10.1093/bioinformatics/btp352
335 Li, H. (2017). *Minimap2: Pairwise alignment for nucleotide sequences.*
336 Manni, M., Berkeley, M. R., Seppey, M., Simão, F. A., & Zdobnov, E. M. (2021). BUSCO
337   Update: Novel and Streamlined Workflows along with Broader and Deeper Phyloge-
338   netic Coverage for Scoring of Eukaryotic, Prokaryotic, and Viral Genomes. *Molecular
339   Biology and Evolution*, *38*(10), 4647–4654. https://doi.org/10.1093/molbev/msab199
340 Mapleson, D., Garcia Accinelli, G., Kettleborough, G., Wright, J., & Clavijo, B. J. (2017). KAT:
341   A K-mer analysis toolkit to quality control NGS datasets and genome assemblies.
342   *Bioinformatics*, *33*(4), 574–576. https://doi.org/10.1093/bioinformatics/btw663
343 Milkman, R., & Beaty, L. (1970). Large-Scale Electrophoretic Studies of Allelic Variation in
344   *Mytilus edulis*. *Biological Bulletin*, *139*, 430.
345 Mölder, F., Jablonski, K., Letcher, B., Hall, M., Tomkins-Tinch, C., Sochat, V., Forster, J., Lee,
346   S., Twardziok, S., Kanitz, A., Wilm, A., Holtgrewe, M., Rahmann, S., Nahnsen, S., &
347   Köster, J. (2021). Sustainable data analysis with Snakemake [version 2; peer review: 2
348   approved]. *F1000Research*, *10*(33). https://doi.org/10.12688/f1000research.29032.2
349 Nakayama, I., Foresti, F., Tewari, R., Schartl, M., & Chourrout, D. (1994). Sex chromosome
350   polymorphism and heterogametic males revealed by two cloned DNA probes in the
351   ZW/ZZ fish Leporinus elongatus. *Chromosoma*, *103*(1), 31–39. https://doi.org/10.
352   1007/BF00364723
353 Popovic, I., & Riginos, C. (2020). Comparative genomics reveals divergent thermal selection
354   in warm and coldtolerant marine mussels. *Molecular Ecology*, *29*(3), 519–535. https:
355   //doi.org/10.1111/mec.15339

Price, M. N., Dehal, P. S., & Arkin, A. P. (2009). FastTree: Computing Large Minimum Evolution Trees with Profiles instead of a Distance Matrix. *Molecular Biology and Evolution*, *26*(7), 1641–1650. https://doi.org/10.1093/molbev/msp077

Queirós, P., Delogu, F., Hickl, O., May, P., & Wilmes, P. (2021). Mantis: Flexible and consensus-driven genome annotation. *GigaScience*, *10*(6), giab042. https://doi.org/10.1093/gigascience/giab042

Quesada, H., Wenne, R., & Skibinski, D. O. F. (1995). Differential introgression of mitochondrial DNA across species boundaries within the marine mussel genus *Mytilus*. *Proceedings of the Royal Society B: Biological Sciences*, *262*(1363), 51–56. https://doi.org/10.1098/rspb.1995.0175

Quesada, H., Zapata, C., & Alvarez, G. (1995). A multilocus allozyme discontinuity in the mussel *Mytilus galloprovincialis*: The interaction of ecological and life-history factors. *Marine Ecology Progress Series*, *116*, 99–115.

Ranallo-Benavidez, T. R., Jaron, K. S., & Schatz, M. C. (2020). GenomeScope 2.0 and Smudgeplot for reference-free profiling of polyploid genomes. *Nature Communications*, *11*(1), 1432. https://doi.org/10.1038/s41467-020-14998-3

Shen, W., Le, S., Li, Y., & Hu, F. (2016). SeqKit: A Cross-Platform and Ultrafast Toolkit for FASTA/Q File Manipulation (Q. Zou, Ed.). *PLOS ONE*, *11*(10), e0163962. https://doi.org/10.1371/journal.pone.0163962

Simon, A., Arbiol, C., Nielsen, E. E., Couteau, J., Sussarellu, R., Burgeot, T., Bernard, I., Coolen, J. W. P., Lamy, J.-B., Robert, S., Skazina, M., Strelkov, P., Queiroga, H., Cancio, I., Welch, J. J., Viard, F., & Bierne, N. (2020). Replicated anthropogenic hybridisations reveal parallel patterns of admixture in marine mussels. *Evolutionary Applications*, *13*(3), 575–599. https://doi.org/10.1111/eva.12879

Simon, A., Fraïsse, C., El Ayari, T., LiautardHaag, C., Strelkov, P., Welch, J. J., & Bierne, N. (2021). How do species barriers decay? Concordance and local introgression in mosaic hybrid zones of mussels. *Journal of Evolutionary Biology*, *34*, 208–223. https://doi.org/10.1111/jeb.13709

Skibinski, D. O. F., Ahmad, M., & Beardmore, J. A. (1978). Genetic evidence of naturally occurring hybrids between *Mytilus edulis* and *M. galloprovincialis*. *32*(2), 354–364. https://doi.org/10.1038/nature01240

Smit, A., Hubley, R., & Green, P. (2013–2015). *RepeatMasker Open-4.0* (Version 4.1.2-p1).

Song, L., & Florea, L. (2015). Rcorrector: Efficient and accurate error correction for Illumina RNA-seq reads. *GigaScience*, *4*(1), 48. https://doi.org/10.1186/s13742-015-0089-y

Stanke, M., Diekhans, M., Baertsch, R., & Haussler, D. (2008). Using native and syntenically mapped cDNA alignments to improve de novo gene finding. *Bioinformatics*, *24*(5), 637–644. https://doi.org/10.1093/bioinformatics/btn013

Trizna, M. (2020). *Assembly_stats 0.1.4* (Version 0.1.4). https://doi.org/10.5281/zenodo.3968775

Vasimuddin Md, S. M., Misra, S., Li, H., & Aluru, S. (2019). *Efficient Architecture-Aware Acceleration of BWA-MEM for Multicore Systems*.

Walker, B. J., Abeel, T., Shea, T., Priest, M., Abouelliel, A., Sakthikumar, S., Cuomo, C. A., Zeng, Q., Wortman, J., Young, S. K., & Earl, A. M. (2014). Pilon: An Integrated Tool for Comprehensive Microbial Variant Detection and Genome Assembly Improvement. *PLOS ONE*, *9*(11), 14.

Weisenfeld, N. I., Kumar, V., Shah, P., Church, D. M., & Jaffe, D. B. (2017). Direct determination of diploid genome sequences. *Genome Research*, *27*(5), 757–767. https://doi.org/10.1101/gr.214874.116

Yang, J.-L., Feng, D.-D., Liu, J., Xu, J.-K., Chen, K., Li, Y.-F., Zhu, Y.-T., Liang, X., & Lu, Y. (2021). Chromosome-level genome assembly of the hard-shelled mussel Mytilus coruscus, a widely distributed species from the temperate areas of East Asia. *Giga-Science*, *10*. https://doi.org/10.1093/gigascience/giab024

Zhang, S. V., Zhuo, L., & Hahn, M. W. (2016). AGOUTI: Improving genome assembly and annotation using transcriptome data. *GigaScience*, *5*(1), 31. https://doi.org/10.1186/s13742-016-0136-3

Supplementary Information

Tables

Table S1: Steps carried out for each version of assembly

Version	Step	
v1	Raw assembly from Supernova	
v2	Supernova assembly using a filtered dataset of reads (section 2.3)	Unused
v3	Assembly with purged duplicates (`purge_dups`) from v3	
v4	Assembly with purged duplicates (`purge_dups`) from v1	
v5	`Agouti` repaired scaffolds from v4	
v6	Assembly with filtered contamination using Blobtoolkit results	
v7	Scaffolded assembly on *M. coruscus*	
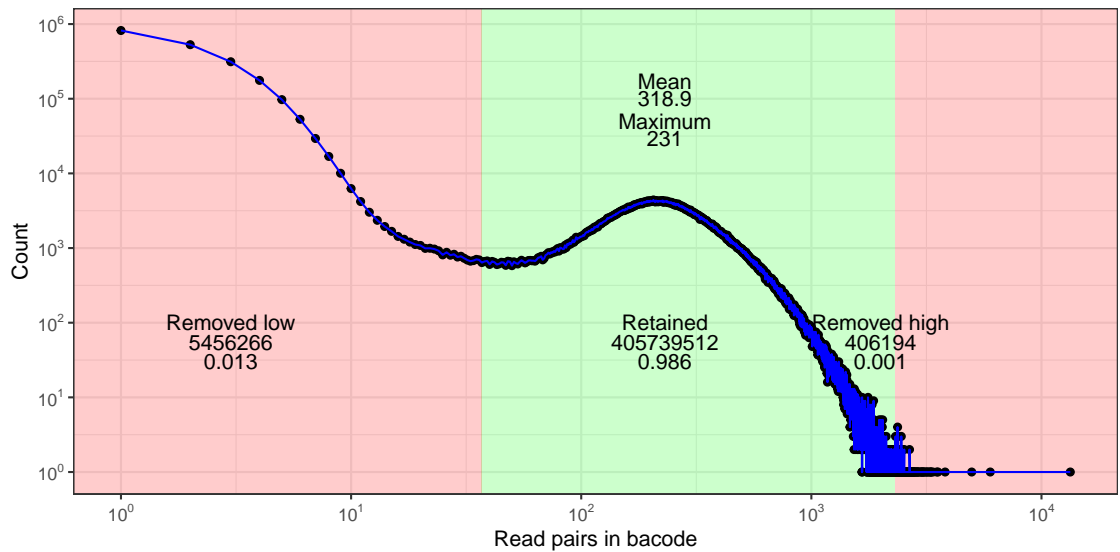
Figures

Figure S1: Histogram of read pairs identified for each 10X barcode for MgalMED. As part of preprocessing step, barcodes for which too few or too many read pairs are associated with each unique barcode are removed from the dataset (red regions).

15
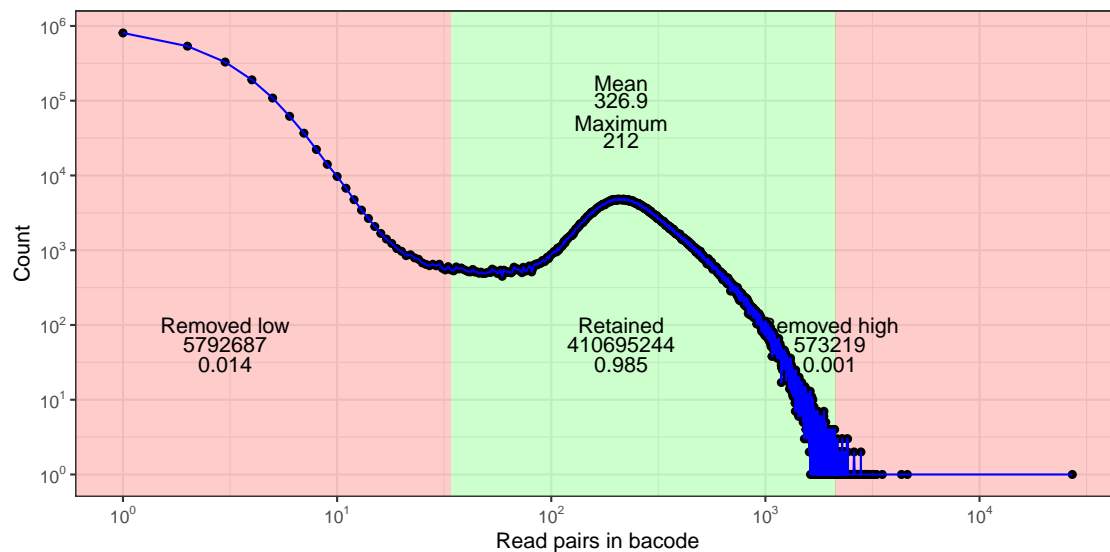
Figure S2: Histogram of read pairs identified for each 10X barcode for MeduEUS. As part of preprocessing step, barcodes for which too few or too many read pairs are associated with each unique barcode are removed from the dataset (red regions).
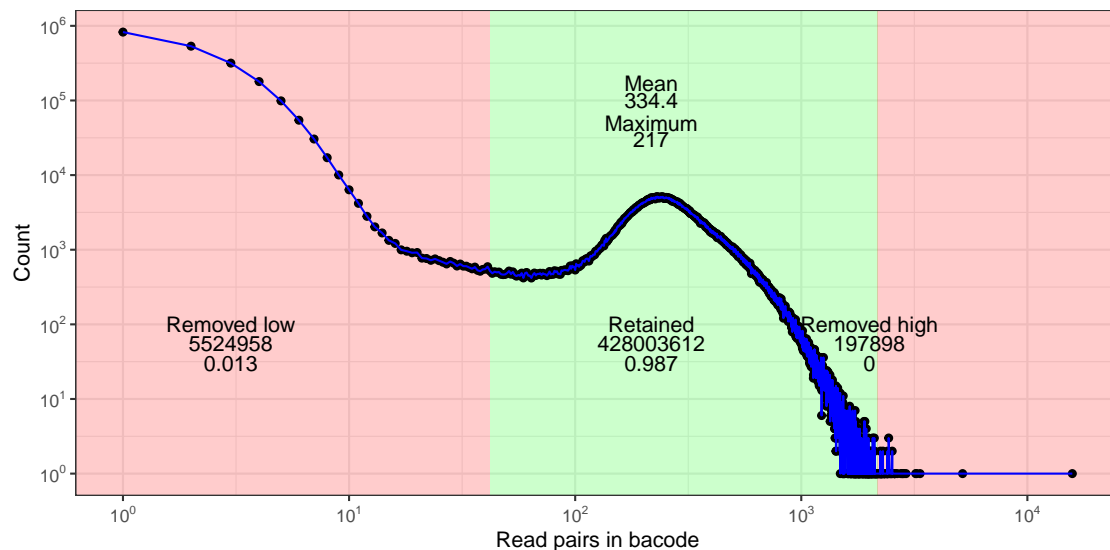
Figure S3: Histogram of read pairs identified for each 10X barcode for MeduEUN. As part of preprocessing step, barcodes for which too few or too many read pairs are associated with each unique barcode are removed from the dataset (red regions).
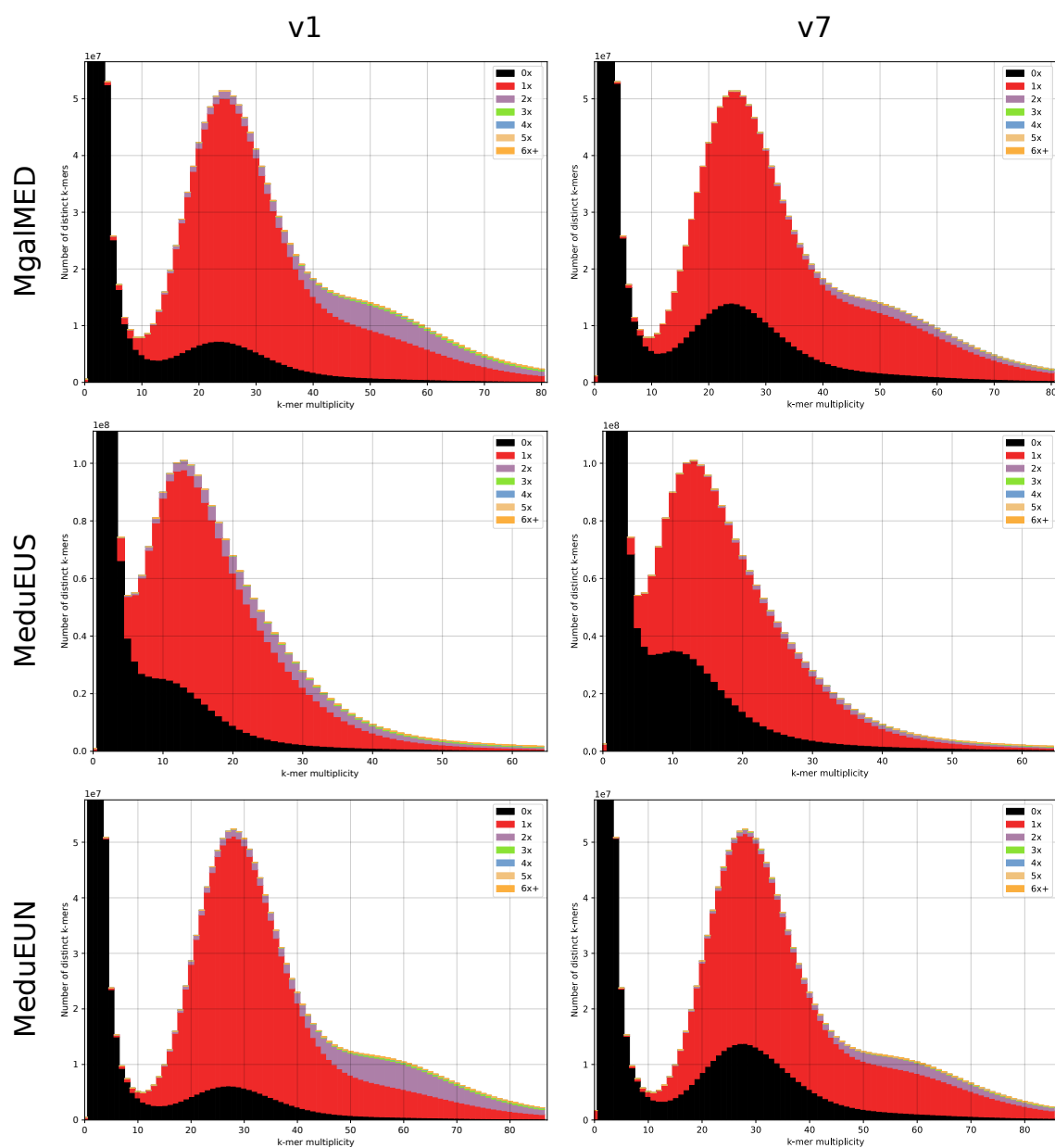
Figure S4: KAT comparison of k–mer spectra between assembly and preprocessed reads. Results are compared between the initial assembly (v1, left column) and the final assembly (v7, right column) for each sample MgalMED, MeduEUS and MeduEUN (from top to bottom).

BUSCO scores Metazoa_odb10 (954 genes)

	Complete single copy	Complete duplicated	Fragmented	Missing
MgalMED_v1	471	293	138	52
MgalMED_v4	598	149	142	65
MgalMED_v5	649	147	102	56
MgalMED_v6	653	137	106	58
MgalMED_v7	727	112	70	45
MeduEUS_v1	601	257	65	31
MeduEUS_v4	660	187	70	37
MeduEUS_v5	680	196	49	29
MeduEUS_v6	687	185	51	31
MeduEUS_v7	726	166	34	28
MeduEUN_v1	431	352	131	40
MeduEUN_v4	570	186	142	56
MeduEUN_v5	621	186	98	49
MeduEUN_v6	618	184	101	51
MeduEUN_v7	701	158	62	33

BUSCO scores Mollusca_odb10 (5295 genes)

	Complete single copy	Complete duplicated	Fragmented	Missing
MgalMED_v1	2222	1133	393	1547
MgalMED_v4	2724	438	429	1704
MgalMED_v5	3102	428	391	1374
MgalMED_v6	3097	423	393	1382
MgalMED_v7	3604	316	346	1029
MeduEUS_v1	2724	705	368	1498
MeduEUS_v4	2971	376	364	1584
MeduEUS_v5	3358	388	328	1221
MeduEUS_v6	3366	374	330	1225
MeduEUS_v7	3824	307	280	884
MeduEUN_v1	2365	1149	412	1369
MeduEUN_v4	2786	539	411	1559
MeduEUN_v5	3040	617	351	1287
MeduEUN_v6	3032	617	354	1292
MeduEUN_v7	3511	528	291	965

categories: Complete single copy, Complete duplicated, Fragmented, Missing

Figure S5: Busco scores on the metazoa_odb10 (left panels) and mollusca_odb10 (right panels) databases for each assembly MgalMED, MeduEUS and MeduEUN (top to bottom panels) across several assembly versions (v1, v4, v5, v6, v7).
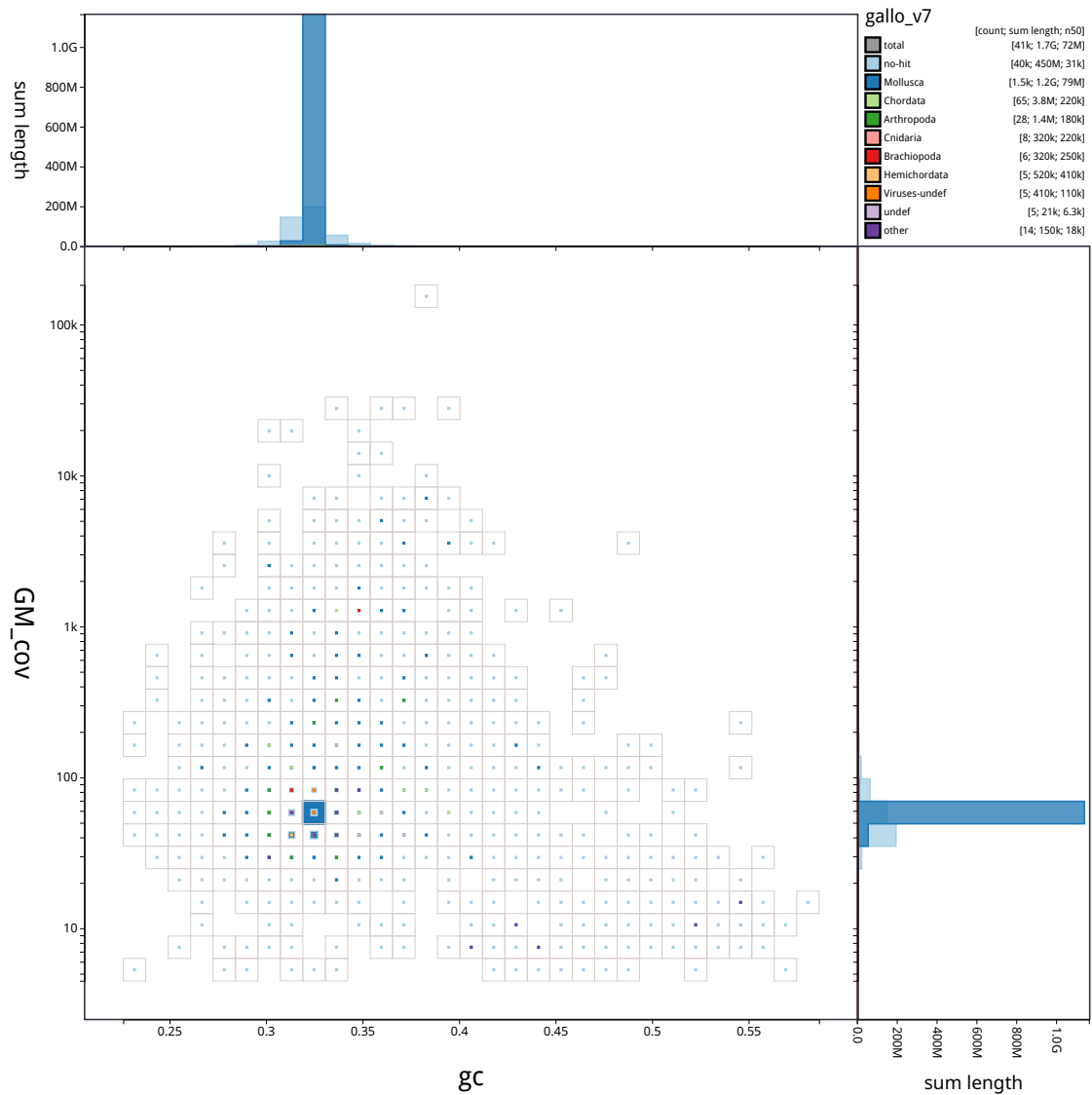
Figure S6: Blobtoolkit blob plot of base coverage in GM against GC proportion for scaffolds in assembly MgalMED_v7. Scaffolds are colored by phylum and binned at a resolution of 30 divisions on each axis. Colored squares within each bin are sized in proportion to the sum of individual scaffold lengths on a square–root scale, ranging from 1,005 to 1,127,105,406. Histograms show the distribution of scaffold length sum along each axis.
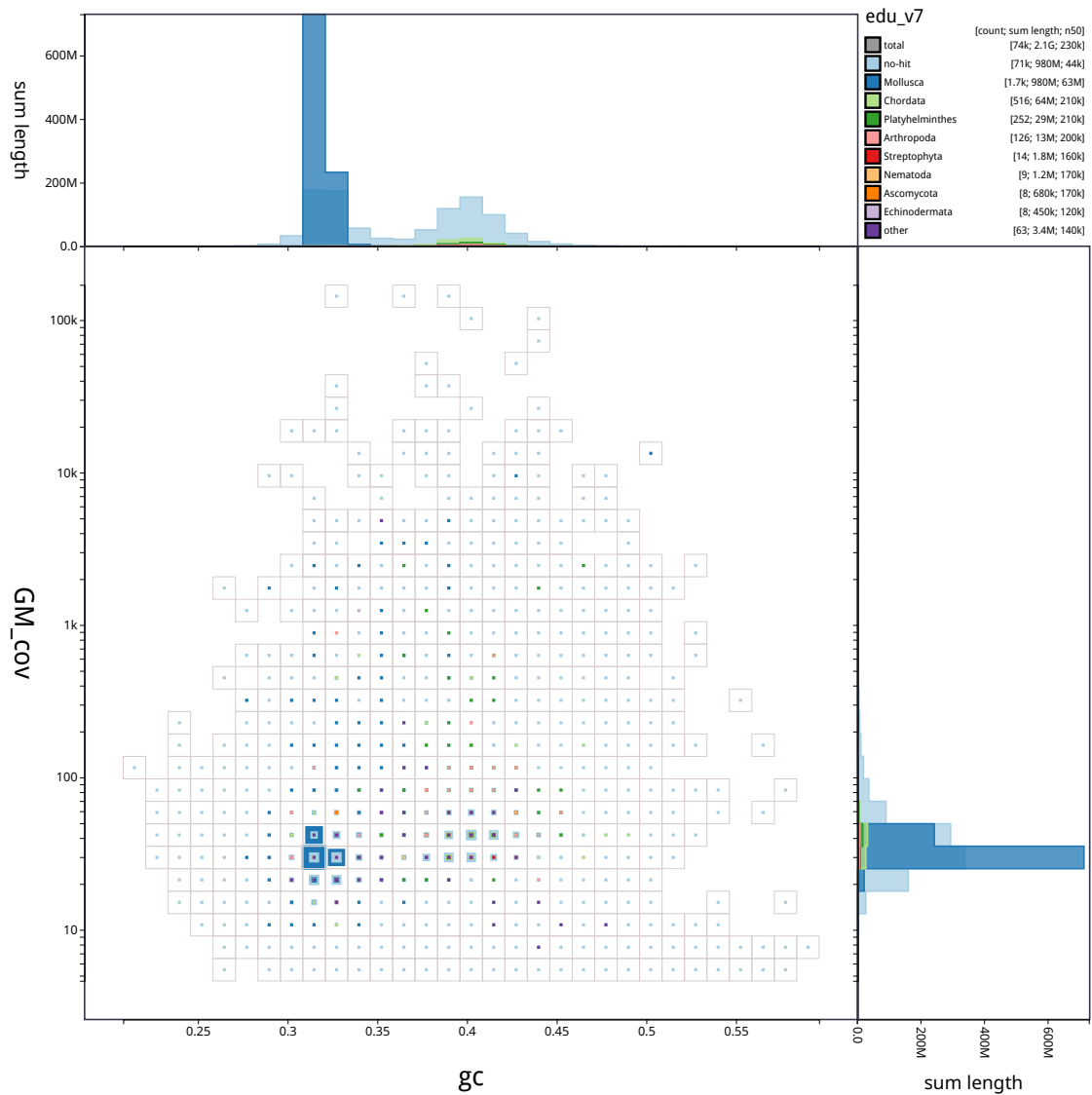
Figure S7: Blobtoolkit blob plot of base coverage in GM against GC proportion for scaffolds in assembly MeduEUS_v7. Scaffolds are colored by phylum and binned at a resolution of 30 divisions on each axis. Colored squares within each bin are sized in proportion to the sum of individual scaffold lengths on a square-root scale, ranging from 987 to 487,517,891. Histograms show the distribution of scaffold length sum along each axis.
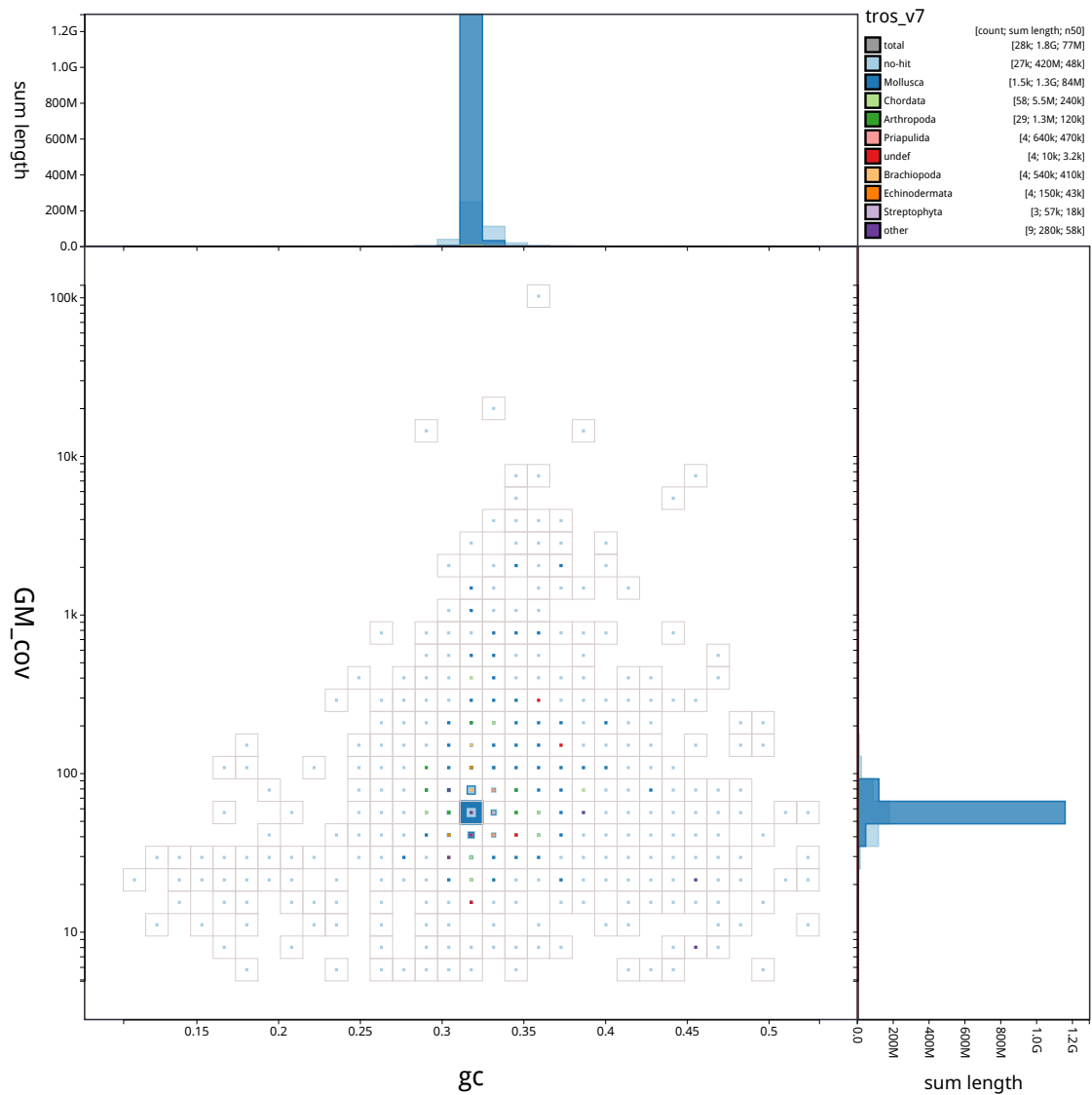
Figure S8: Blobtoolkit blob plot of base coverage in GM against GC proportion for scaffolds in assembly MeduEUN_v7. Scaffolds are colored by phylum and binned at a resolution of 30 divisions on each axis. Colored squares within each bin are sized in proportion to the sum of individual scaffold lengths on a square-root scale, ranging from 1,011 to 1,136,301,196. Histograms show the distribution of scaffold length sum along each axis.
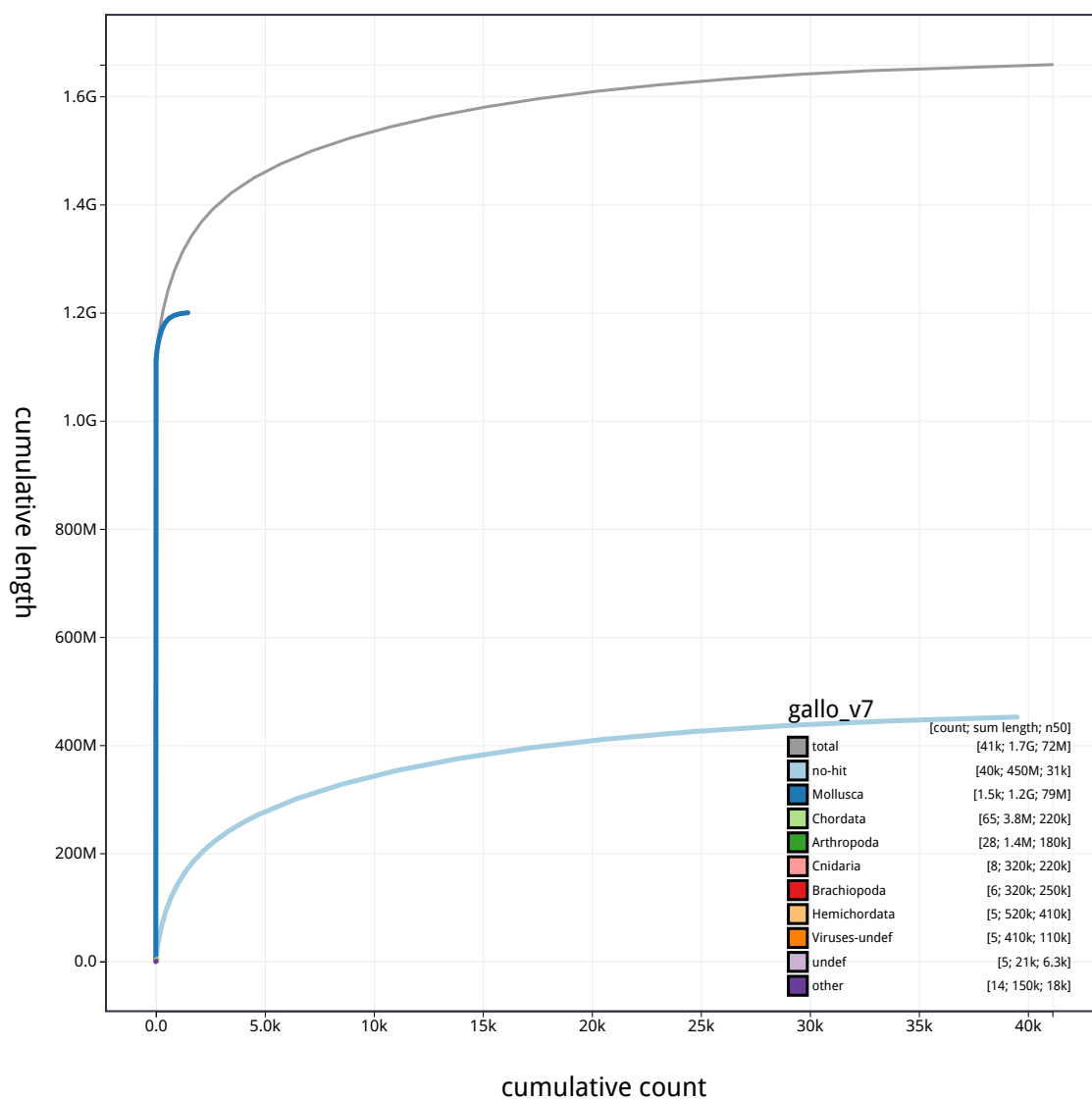
Figure S9: Blobtoolkit cumulative scaffold length for assembly MgalMED_v7. The gray line shows cumulative length for all scaffolds. Colored lines show cumulative lengths of scaffolds assigned to each phylum using the bestsumorder taxrule.
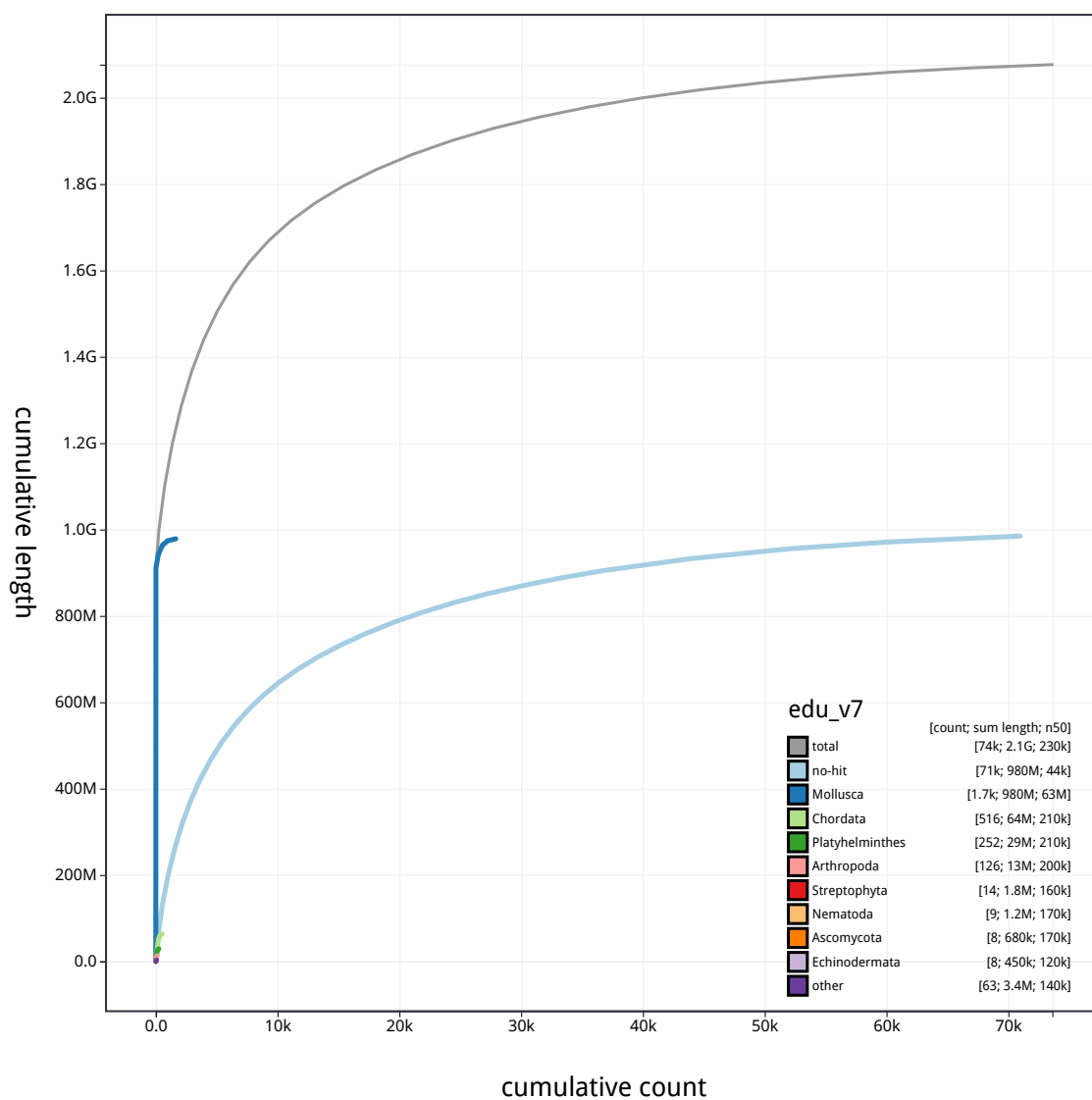
Figure S10: Blobtoolkit cumulative scaffold length for assembly MeduEUS_v7. The gray line shows cumulative length for all scaffolds. Colored lines show cumulative lengths of scaffolds assigned to each phylum using the bestsumorder taxrule.
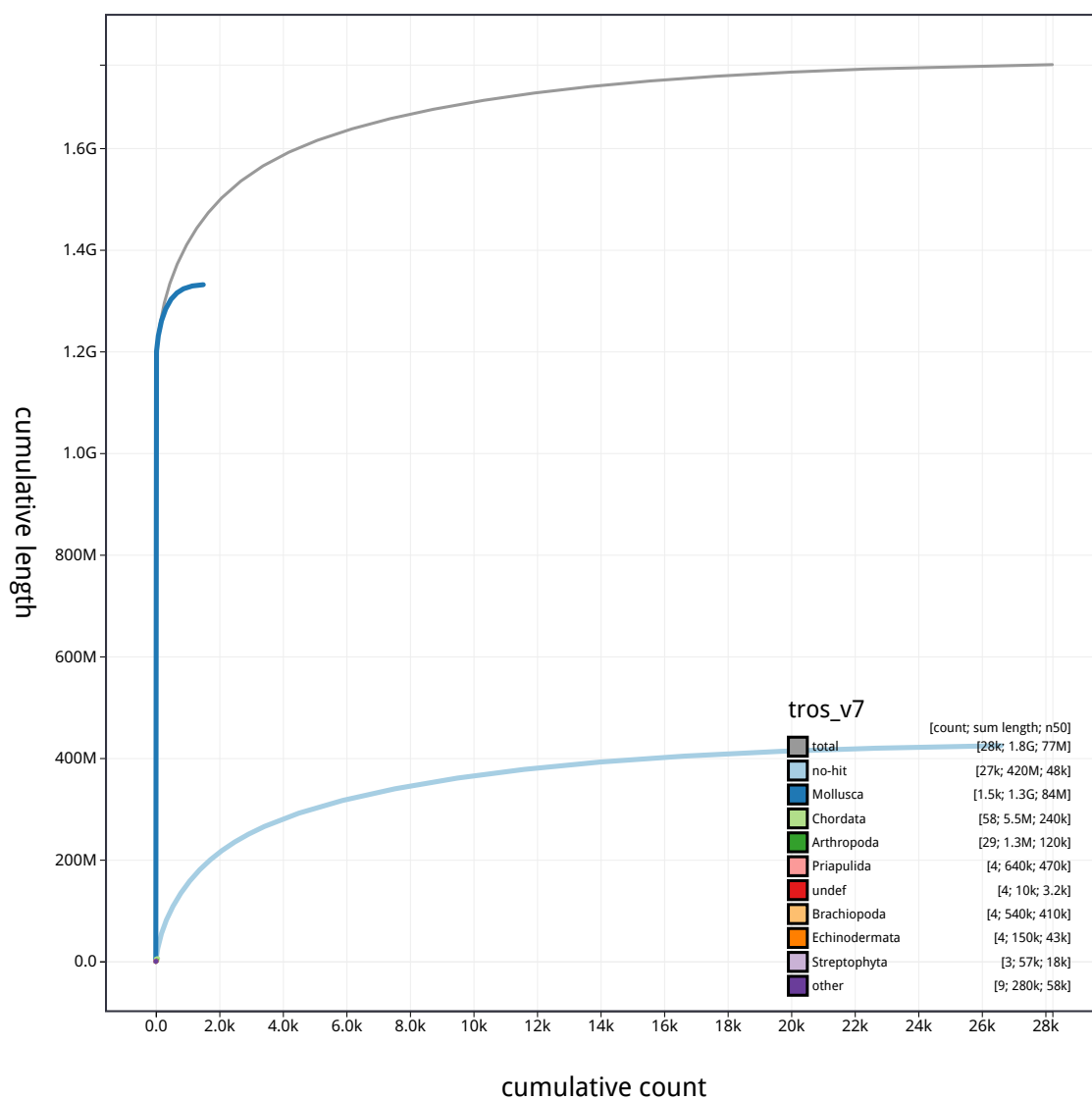
Figure S11: Blobtoolkit cumulative scaffold length for assembly MeduEUN_v7. The gray line shows cumulative length for all scaffolds. Colored lines show cumulative lengths of scaffolds assigned to each phylum using the bestsumorder taxrule.
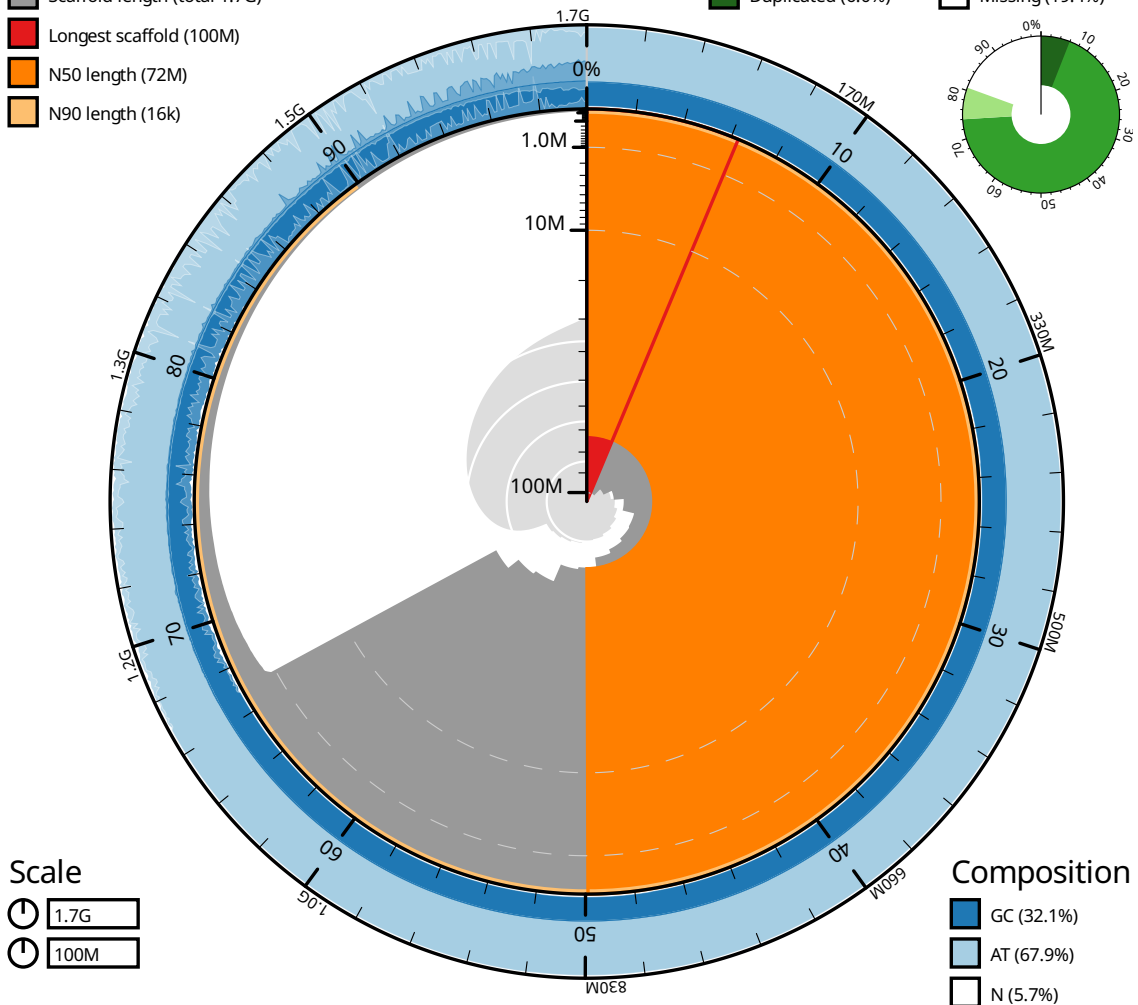
Figure S12: Blobtoolkit snail plot summary of assembly statistics for assembly MgalMED_v7. The main plot is divided into 1,000 size-ordered bins around the circumference with each bin representing 0.1% of the 1,658,656,017 bp assembly. The distribution of scaffold lengths is shown in dark gray with the plot radius scaled to the longest scaffold present in the assembly (104,729,878 bp, shown in red). Orange and pale-orange arcs show the N50 and N90 scaffold lengths (71,952,646 and 16,011 bp), respectively. The pale gray spiral shows the cumulative scaffold count on a log scale with white scale lines showing successive orders of magnitude. The blue and pale-blue area around the outside of the plot shows the distribution of GC, AT and N percentages in the same bins as the inner plot. A summary of complete, fragmented, duplicated and missing BUSCO genes in the mollusca_odb10 set is shown in the top right.
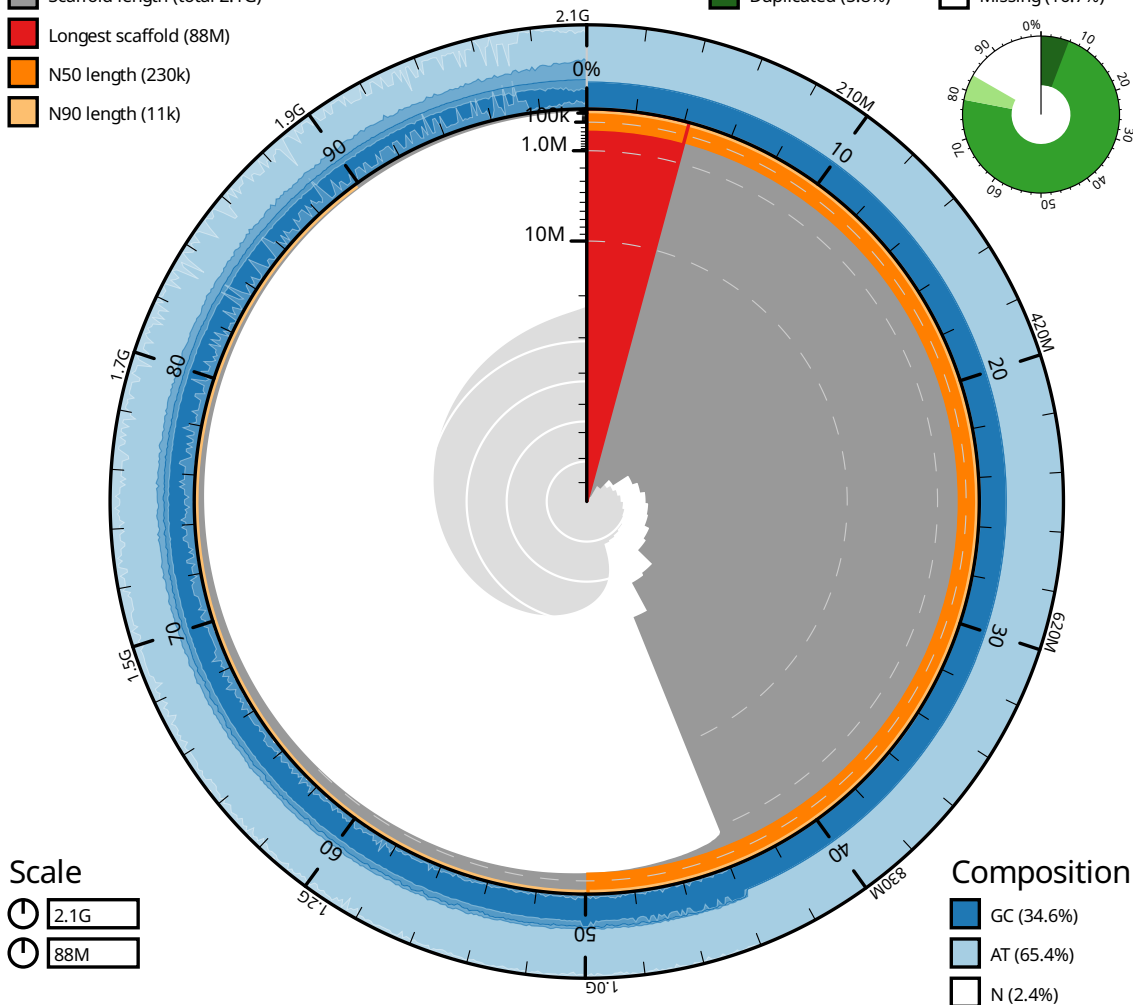
Figure S13: Blobtoolkit snail plot summary of assembly statistics for assembly MeduEUS_v7. The main plot is divided into 1,000 size-ordered bins around the circumference with each bin representing 0.1% of the 2,076,685,641 bp assembly. The distribution of scaffold lengths is shown in dark gray with the plot radius scaled to the longest scaffold present in the assembly (88,305,666 bp, shown in red). Orange and pale-orange arcs show the N50 and N90 scaffold lengths (228,263 and 10,773 bp), respectively. The pale gray spiral shows the cumulative scaffold count on a log scale with white scale lines showing successive orders of magnitude. The blue and pale-blue area around the outside of the plot shows the distribution of GC, AT and N percentages in the same bins as the inner plot. A summary of complete, fragmented, duplicated and missing BUSCO genes in the mollusca_odb10 set is shown in the top right.
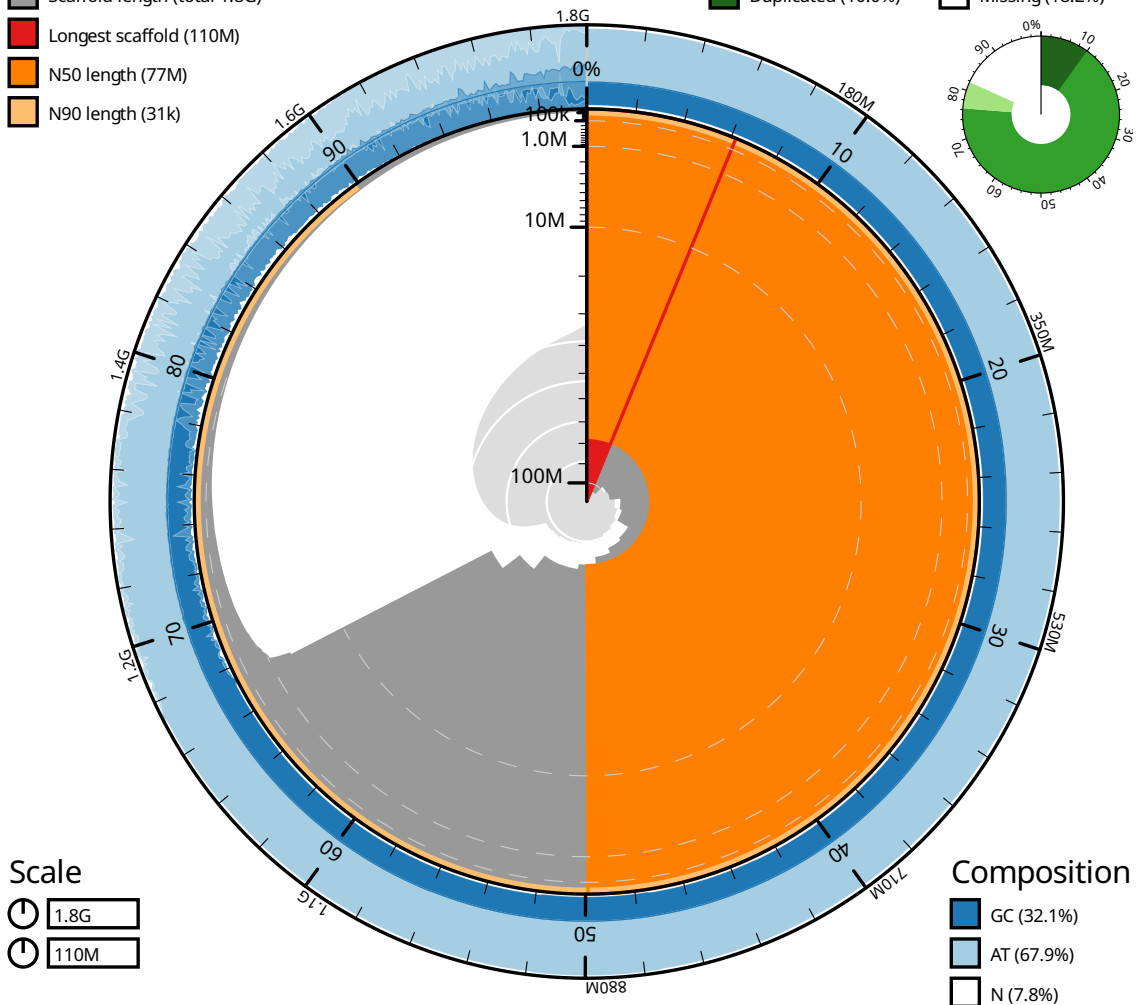
Figure S14: Blobtoolkit snail plot summary of assembly statistics for assembly MeduEUN_v7. The main plot is divided into 1,000 size-ordered bins around the circumference with each bin representing 0.1% of the 1,764,246,486 bp assembly. The distribution of scaffold lengths is shown in dark gray with the plot radius scaled to the longest scaffold present in the assembly (110,194,685 bp, shown in red). Orange and pale-orange arcs show the N50 and N90 scaffold lengths (77,102,752 and 30,649 bp), respectively. The pale gray spiral shows the cumulative scaffold count on a log scale with white scale lines showing successive orders of magnitude. The blue and pale-blue area around the outside of the plot shows the distribution of GC, AT and N percentages in the same bins as the inner plot. A summary of complete, fragmented, duplicated and missing BUSCO genes in the mollusca_odb10 set is shown in the top right.

Table S2: RepeatMasker results.

			MgalMED	MeduEUS	MeduEUN
Retroelements			17.89%	26.39%	17.91%
	SINEs:		0.03%	0.04%	0.03%
		Penelope	5.16%	5.31%	5.15%
	LINEs:		9.71%	13.83%	9.83%
		CRE/SLACS	0.00%	0.23%	0.00%
		L2/CR1/Rex	0.85%	3.86%	0.85%
		R1/LOA/Jockey	0.19%	0.14%	0.20%
		R2/R4/NeSL	0.04%	0.06%	0.04%
		RTE/Bov-B	1.60%	2.88%	1.66%
		L1/CIN4	0.57%	0.32%	0.53%
	LTR elements:		8.15%	12.52%	8.04%
		BEL/Pao	1.34%	3.18%	1.36%
		Ty1/Copia	0.08%	0.07%	0.09%
		Gypsy/DIRS1	3.37%	5.38%	3.34%
		Retroviral	0.01%	0.01%	0.01%
DNA transposons			2.09%	3.44%	2.06%
		hobo-Activator	0.18%	0.62%	0.18%
		Tc1-IS630-Pogo	0.19%	0.92%	0.18%
		En-Spm	0.00%	0.00%	0.00%
		MuDR-IS905	0.00%	0.00%	0.00%
		PiggyBac	0.02%	0.36%	0.03%
		Tourist/Harbinger	0.06%	0.04%	0.06%
		Other (Mirage, P-element, Transib)	0.00%	0.00%	0.00%
Rolling-circles			0.14%	0.10%	0.13%
Unclassified:			36.50%	30.64%	34.85%
Total interspersed repeats:			56.48%	60.47%	54.82%
Small RNA:			0.03%	0.09%	0.03%
Satellites:			0.04%	0.03%	0.04%
Simple repeats:			0.44%	0.35%	0.42%
Low complexity:			0.09%	0.07%	0.09%